

Glycan Recognition
Editor's Choice

Helicobacter pylori induces intracellular galectin-8 aggregation around damaged lysosomes within gastric epithelial cells in a host O-glycan-dependent manner

Fang-Yen Li², I-Chun Weng³, Chun-Hung Lin⁴, Mou-Chieh Kao⁵,
Ming-Shiang Wu⁶, Huan-Yuan Chen³, and Fu-Tong Liu^{3,7,1}

²Graduate Institute of Immunology, College of Medicine, National Taiwan University, Taipei 10617, Taiwan, ³Institute of Biomedical Sciences, and ⁴Institute of Biological Chemistry, Academia Sinica, Taipei 115, Taiwan, ⁵Institute of Molecular Medicine, National Tsing Hua University, Hsinchu 30013, Taiwan, ⁶Department of Internal Medicine, National Taiwan University Hospital 100, Taipei, Taiwan, and ⁷Department of Dermatology, School of Medicine, University of California-Davis, Sacramento, CA 95817, USA

¹To whom correspondence should be addressed: Tel: +886-2-2652-3056; e-mail: ftliu@ibms.sinica.edu.tw

Received 20 August 2018; Revised 19 September 2018; Editorial decision 29 September 2018; Accepted 5 October 2018

Abstract

Galectin-8, a beta-galactoside-binding lectin, is upregulated in the gastric tissues of rhesus macaques infected with *Helicobacter pylori*. In this study, we found that *H. pylori* infection triggers intracellular galectin-8 aggregation in human-derived AGS gastric epithelial cells, and that these aggregates colocalize with lysosomes. Notably, this aggregation is markedly reduced following the attenuation of host O-glycan processing. This indicates that *H. pylori* infection induces lysosomal damage, which in turn results in the accumulation of cytosolic galectin-8 around damaged lysosomes through the recognition of exposed vacuolar host O-glycans. *H. pylori*-induced galectin-8 aggregates also colocalize with autophagosomes, and galectin-8 ablation reduces the activation of autophagy by *H. pylori*. This suggests that galectin-8 aggregates may enhance autophagy activity in infected cells. We also observed that both autophagy and NDP52, an autophagy adapter, contribute to the augmentation of galectin-8 aggregation by *H. pylori*. Additionally, vacuolating cytotoxin A, a secreted *H. pylori* cytotoxin, may contribute to the increased galectin-8 aggregation and elevated autophagy response in infected cells. Collectively, these results suggest that *H. pylori* promotes intracellular galectin-8 aggregation, and that galectin-8 aggregation and autophagy may reciprocally regulate each other during infection.

Key words: autophagy, galectin-8, glycan, *Helicobacter pylori*, lysosome

Introduction

Helicobacter pylori is a Gram-negative, flagellated, microaerophilic bacterium mainly found in the stomach. Notably, at least half of the world's population is colonized by this microorganism. Infection by *H. pylori* is known to cause gastritis, and some infected individuals

may develop peptic ulcers and gastric adenocarcinoma (Atherton 2006). The differences in these clinical outcomes are likely associated with bacterial virulence factors, host genetic factors, and the interplay between host and bacteria (Figueiredo et al. 2002; Izzotti et al. 2007; Jones et al. 2010). The best characterized *H. pylori*

virulence factors are cytotoxin-associated gene A (CagA) and vacuolating cytotoxin A (VacA) (Jones et al. 2010). CagA is translocated into the cytoplasm of gastric epithelial cells through the type IV secretion system after *H. pylori* attachment (Backert et al. 2000; Odenbreit et al. 2000). Once being delivered into the cytosol, CagA exerts multiple effects in host cells, including enhancement of cell migration and proinflammatory cytokine production, as well as disruption of cell polarity (Jones et al. 2010). VacA is secreted by *H. pylori* and characterized by its ability to induce large vacuole formation in host cells with an as yet unidentified purpose (de Bernard et al. 1997). VacA also mediates apoptosis by targeting mitochondria and inducing cytochrome c release (Palframan et al. 2012).

Autophagy is important for maintaining cellular homeostasis under different stress conditions, such as cell starvation and damage of cytosolic organelles (Mizushima 2007; Filomeni et al. 2015). Autophagy is initiated by the formation of an isolation membrane or phagophore, which elongates and sequesters cytoplasmic materials to form vesicles called autophagosomes (Kaur and Debnath 2015). Complete autophagosome formation requires atg5-atg12 conjugation as well as LC3 modification (Yang and Klionsky 2010; Walczak and Martens 2013; Kaur and Debnath 2015). Autophagosomes fuse with lysosomes to form autolysosomes, followed by digestion of the luminal components by lysosomal hydrolases (Kaur and Debnath 2015). In addition to maintaining cellular homeostasis, autophagy regulates innate immunity against intracellular bacteria. When cells are confronted with invasive pathogens, the pathogens are recognized by innate immune receptors, such as Toll-like receptors, to activate autophagy in order to eliminate these microorganisms (Delgado et al. 2009; Deretic et al. 2013). While *H. pylori* is an extracellular bacterium, it also triggers an autophagic response in gastric epithelial cells (Terebiznik et al. 2009). Among the virulence factors of *H. pylori*, VacA cytotoxin is critical for elevating autophagy activity in host cells upon infection (Terebiznik et al. 2009; Kim et al. 2018).

Lysosomes are membrane-enclosed organelles found in eukaryotic cells. They contain numerous hydrolytic enzymes to degrade a variety of biomolecules for recycling and eliminate microorganisms internalized into host cells. Upon lysosomal damage, lysosomal contents may leak into the cytosol to induce apoptosis (Aits and Jaattela 2013). A panel of distinct agents can trigger lysosomal disruption, including lysosomotropic detergents, reactive oxygen species (ROS), viral proteins, and bacterial/fungal toxins (Aits and Jaattela 2013). As for *H. pylori*, it remains undetermined whether infection by this bacterium alters lysosomal integrity in host cells.

Galectins are a family of animal lectins that bind to beta-galactoside-containing glycoconjugates through their carbohydrate-recognition domain(s) (Barondes et al. 1994). They have been linked to a wide variety of biological functions involved in physiological and pathological processes (Liu et al. 2012). Notably, owing to their carbohydrate-binding capacity and presence in the cytosol, galectins are now well-recognized as intracellular sensors of vacuole lysis. Once being internalized into host cells, some invasive bacteria, such as *Salmonella typhimurium* and *Listeria monocytogenes*, can disrupt vacuoles that they are initially confined in. This leads to the exposure of vacuolar luminal glycans to the cytosol and the subsequent binding of cytosolic galectins to the exposed glycans, resulting in the formation of intracellular galectin aggregates (Paz et al. 2010; Thurston et al. 2012). Galectin-1 can detect lysosomal rupture, whereas galectin-3, -8 and -9 can sense damage to endosomes or lysosomes (Thurston et al. 2012; Weng et al. 2018). Galectin-8 has been shown to promote autophagic clearance of bacteria-containing

intracellular vesicles through the recruitment of NDP52, an autophagy adapter (Thurston et al. 2012). Therefore, galectin-8 serves as a danger receptor to defend against bacterial invasion by monitoring the integrity of endocytic vesicles.

Galectin-8 mRNA expression is elevated in gastric tissues of rhesus macaques infected with *H. pylori* (Huff et al. 2004). The current study aimed to investigate the role of galectin-8 in gastric epithelial cells upon exposure to *H. pylori*. We observed an increase in intracellular galectin-8 aggregation in *H. pylori*-infected gastric epithelial cells, which was attributable to lysosomal destruction by *H. pylori* and dependent on host O-glycans. Furthermore, the functional role of galectin-8 in *H. pylori*-mediated autophagy in gastric epithelial cells was investigated. *H. pylori*-induced galectin-8 aggregates colocalized with autophagosomes, and galectin-8 depletion downregulated *H. pylori*-driven autophagy activation. We also demonstrated that autophagy contributed to the increase in galectin-8 aggregation after infection. Therefore, *H. pylori*-induced galectin-8 aggregation and autophagy reciprocally regulate each other during *H. pylori* infection.

Results

H. pylori infection promotes intracellular galectin-8 aggregation in AGS gastric epithelial cells

In AGS human gastric epithelial cells, we observed an increase in galectin-8 mRNA extent after infection with *H. pylori* for 24 h (Figure 1A). However, at the protein level, galectin-8 was mildly downregulated at this time point postinfection (Figure 1B). Shiga toxin produced by enterohemorrhagic *Escherichia coli* was reported to cause galectin-3 depletion in intestinal epithelial cells by increasing galectin-3 secretion (Laiko et al. 2010). *H. pylori* exposure enhanced galectin-8 release from AGS cells (Supplementary data, Figure S1A), thus possibly contributing to reduced galectin-8 in infected cells. Galectin-3 is known to be capable of associating with *H. pylori* (Fowler et al. 2006), and we demonstrated a similar functional ability of galectin-8 to bind *H. pylori* (Supplementary data, Figure S1B).

We also employed immunofluorescence microscopy to examine galectin-8 in AGS cells before and after incubation with *H. pylori*. Limited intracellular galectin-8 aggregates were observed in some uninfected cells, whilst *H. pylori* facilitated this aggregation phenomenon (Figure 1C). A time-course experiment was conducted to examine temporal changes in galectin-8 aggregation in infected cells. AGS cells were treated with *H. pylori* for 2, 5 or 8 h or left untreated, and the average number of galectin-8 aggregates per cell was determined after microscopic analysis. As revealed in Figure 1D and E, there was a gradual increase in galectin-8 aggregation during this 8-h infection period. Additionally, the effect of multiplicity of infection (moi) on *H. pylori*-induced galectin-8 aggregation was examined. Infection with different doses of *H. pylori* revealed a positive correlation between galectin-8 aggregation and bacterial moi (Figure 1F and G). The results suggest the extent of intracellular galectin-8 aggregation reflects the severity of infection in host cells.

H. pylori-induced intracellular galectin-8 aggregation is related to enhanced lysosomal damage

Next, we determined whether *H. pylori*-induced galectin-8 aggregates colocalize with endocytic vesicles, including endosomes and lysosomes. These aggregates demonstrated a more pronounced colocalization with LAMP1-positive lysosomes than with EEA1-positive

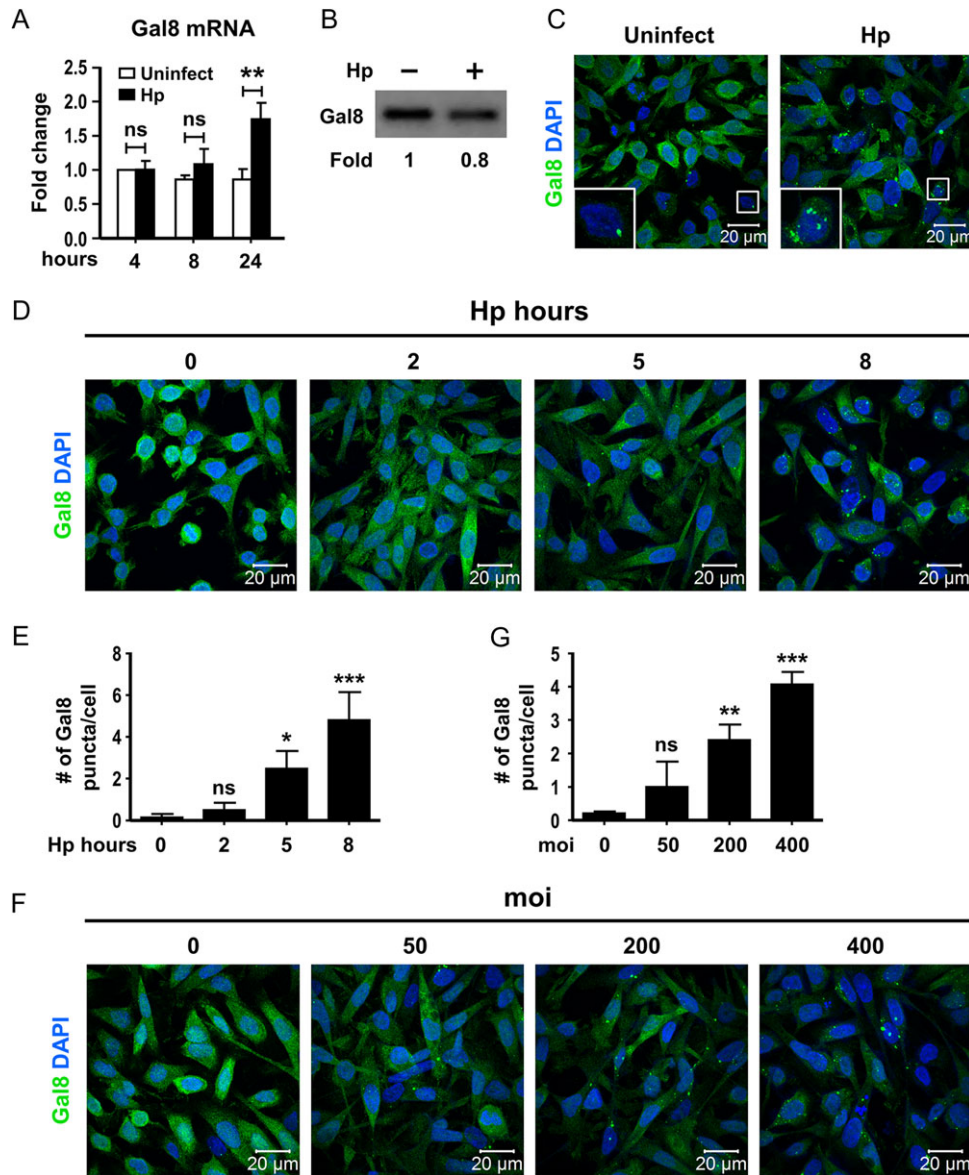


Fig. 1. *H. pylori* infection induces an increase in intracellular galectin-8 aggregation in AGS gastric epithelial cells. (A) AGS cells were infected with *H. pylori* 26695 (moi = 200) for indicated hours and then lysed to analyze galectin-8 mRNA levels by quantitative PCR. Data represent the means ± SD of three independent experiments. (B) Cells were infected with *H. pylori* 26695 (moi = 200) for 24 h and then lysed. Cell lysates were incubated with lactosyl-Sepharose. The bound proteins were eluted and resolved by SDS-PAGE followed by immunoblotting with anti-galectin-8 antibody. Each lane represents galectin-8 from 450 μg total proteins. The relative amounts of galectin-8 are indicated. (C) After infection with *H. pylori* 26695 (moi = 200) for 8 h, cells were stained with mouse anti-galectin-8 antibody and an anti-mouse Alexa 488 (green) fluorescent antibody. DAPI stains nuclei and bacteria. Scale bar, 20 μm. (D) After infection with *H. pylori* 26695 (moi = 200) for indicated hours, cells and bacteria were stained as in (C). Scale bar, 20 μm. (E) Quantitative analysis of galectin-8 puncta per cell from three independent experiments as described in (D). For each experiment, at least 100 cells were counted at each time point. Values represent means ± SD. (F) After infection with *H. pylori* 26695 at indicated moi for 5 h, cells and bacteria were stained as in (C). Scale bar, 20 μm. (G) Quantitative analysis of galectin-8 puncta per cell from three independent experiments as described in (F). For each experiment, at least 100 cells were counted for each condition. Values represent means ± SD. **P* < 0.05, ***P* < 0.01, ****P* < 0.001. Hp, *H. pylori*; ns, not significant; moi, multiplicity of infection.

endosomes in infected cells (Figure 2A). Because galectin-8 is a marker of vacuolar rupture (Thurston et al. 2012; Jia et al. 2018), this observation indicates that *H. pylori* infection may induce lysosomal disruption in gastric epithelial cells. To confirm this, we monitored cytosolic cathepsin B activity in infected cells. Lysosomal damage induces cathepsin proteases to translocate from lysosomes to the cytosol, leading to an increase in cytosolic cathepsins (Boya and Kroemer 2008). Cytosolic cathepsin B activity was augmented after *H. pylori* challenge (Figure 2B), implying increased lysosomal

injury in *H. pylori*-infected cells. Therefore, *H. pylori*-mediated galectin-8 aggregation may be related to augmented lysosomal damage.

Host O-glycans are crucial for *H. pylori*-induced galectin-8 aggregation

Since cytosolic galectin-8 develops intracellular aggregates following recognition of intravacuolar host glycans (Thurston et al. 2012), we

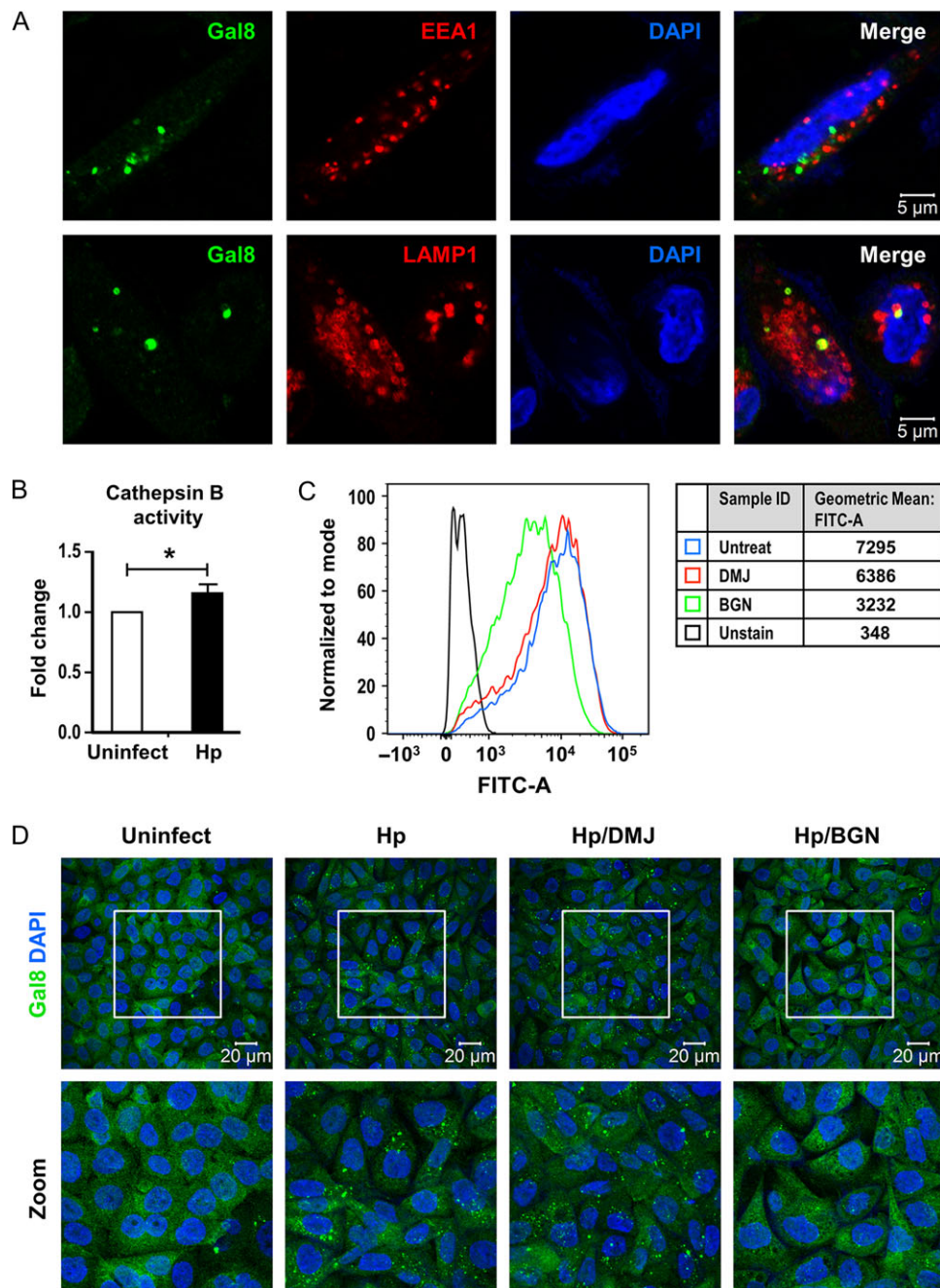


Fig. 2. *H. pylori*-induced galectin-8 aggregation is attributed to enhanced lysosomal damage in infected cells. (A) Cells were infected with *H. pylori* 26695 (moi = 200) for 8 h, stained with anti-galectin-8, anti-EEA1 or anti-LAMP1 antibodies, and then appropriate fluorescence-labeled secondary antibodies. DAPI stains nuclei and bacteria. Yellow color represents colocalization of galectin-8 with LAMP1. Scale bar, 5 μ m. 11.17% of galectin-8 puncta exhibited EEA1 staining signal, whereas 77.68% of galectin-8 puncta showed LAMP1 staining signal. For each double staining, 20 images were collected, and more than 530 galectin-8 puncta were analyzed. (B) Relative cathepsin B activity in cytosolic extracts isolated from cells infected with *H. pylori* 26695 (moi = 400) for 16 h. Data represent the means \pm SD of three independent experiments. (C) Cells were treated with 1 mM DMJ or 10 mM BGN for 24 h, stained with fluorescein isothiocyanate (FITC)-labeled recombinant human galectin-8, and then analyzed by flow cytometry. The representative image and geometric mean fluorescence intensity are shown on the left and right, respectively. (D) Cells were pretreated with indicated drugs as described in (C) and infected with *H. pylori* 26695 (moi = 200) for additional 8 h. Cells and bacteria were then stained as in Figure 1C. "Zoom" depicts a magnified picture of the boxed region. Scale bar, 20 μ m. * P < 0.05. EEA1, early endosome antigen 1; LAMP1, lysosomal-associated membrane protein 1; Hp, *H. pylori*; DMJ, 1-deoxymannojirimycin; BGN, benzyl 2-acetamido-2-deoxy- α -D-galactopyranoside.

assessed whether *H. pylori*-elicited galectin-8 aggregates are formed in a similar way. 1-deoxymannojirimycin (DMJ) and benzyl 2-acetamido-2-deoxy- α -D-galactopyranoside (BGN) were utilized to disrupt

the biosynthesis of host N- and O-glycans, respectively. DMJ, a mannosidase I inhibitor, blocks host N-glycan maturation and thereby reduces L-phytohemagglutinin (PHA-L) lectin binding to

treated cells (Bagriacik et al. 1996). BGN disturbs host O-glycan biosynthesis via abolishing GalNAc-O-Ser/Thr elongation and consequently enhances Peanut agglutinin (PNA) lectin binding signal on treated cells (Suzuki and Abe 2014). First, we confirmed that each drug could attenuate host glycan processing by demonstrating a decrease or increase in cell-surface glycans recognized by PHA-L and PNA lectins, respectively (Supplementary data, Figure S2). In addition, the binding of recombinant galectin-8 to drug-treated cells was also analyzed, and the levels of cell-surface glycans recognized by galectin-8 were markedly decreased in BGN- but not DMJ-incubated cells (Figure 2C). We then pretreated cells with DMJ or BGN for 24 h, followed by incubation with *H. pylori* for an additional 8 h. Microscopic analysis revealed that treatment with BGN rather than DMJ profoundly reduced *H. pylori*-mediated galectin-8 aggregation in infected cells (Figure 2D). These observations suggest that galectin-8 aggregation is dependent on host O-glycans, and support the idea that galectin-8 aggregates in *H. pylori*-infected cells develop following the recognition of lysosomal damage. Therefore, *H. pylori* infection promotes lysosomal damage in host cells, thereby facilitating the access of cytosolic galectin-8 to glycans initially confined in the lysosomal lumen, to form aggregates.

Galectin-8 upregulates autophagy response in *H. pylori*-infected cells

Galectin-8 aggregates induced by vacuolar damage were known to enhance autophagy activation during bacterial invasion (Thurston et al. 2012). We observed that *H. pylori*-induced galectin-8

aggregates colocalized with autophagosomes (indicated by the presence of LC3) and NDP52, an autophagy receptor (Figure 3A). We thus suspected that galectin-8 might regulate *H. pylori*-mediated autophagy in infected cells. To address this, galectin-8 knockdown cells were generated by lentiviral-mediated shRNA transduction (Figure 3B). Cellular autophagy activity was determined by analyzing LC3-II levels in bafilomycin A1 (an autophagosome-lysosome fusion inhibitor)-treated cells via immunoblotting. Galectin-8 depletion attenuated *H. pylori*-induced increase in LC3-II levels after infection (Figure 3C and D), suggesting a role of galectin-8 in upregulating the cellular autophagy response during *H. pylori* coculture.

Autophagy enhances galectin-8 aggregation in *H. pylori*-infected cells

Under some situations, autophagy can mediate lysosomal destruction (Gonzalez et al. 2012; Wang et al. 2015; Hernandez-Tiedra et al. 2016; Yao et al. 2016; Liu et al. 2017; Wu et al. 2017). Therefore, we investigated whether autophagy contributes to galectin-8 aggregation during *H. pylori* infection. Autophagy inhibition by 3-methyladenine (3-MA) treatment suppressed *H. pylori*-mediated galectin-8 aggregation (Figure 4A and B), implying that autophagy can expedite galectin-8 aggregation during *H. pylori* infection. To confirm this, atg5-knockout AGS cells were generated using CRISPR/Cas9 (Figure 4C). We found atg5-knockout cells (#7 and #12) exhibited lower levels of galectin-8 aggregation compared with atg5-expressing cells (#8 and #11) after exposure to *H. pylori* (Figure 4D and E). This reinforces the observation that autophagy

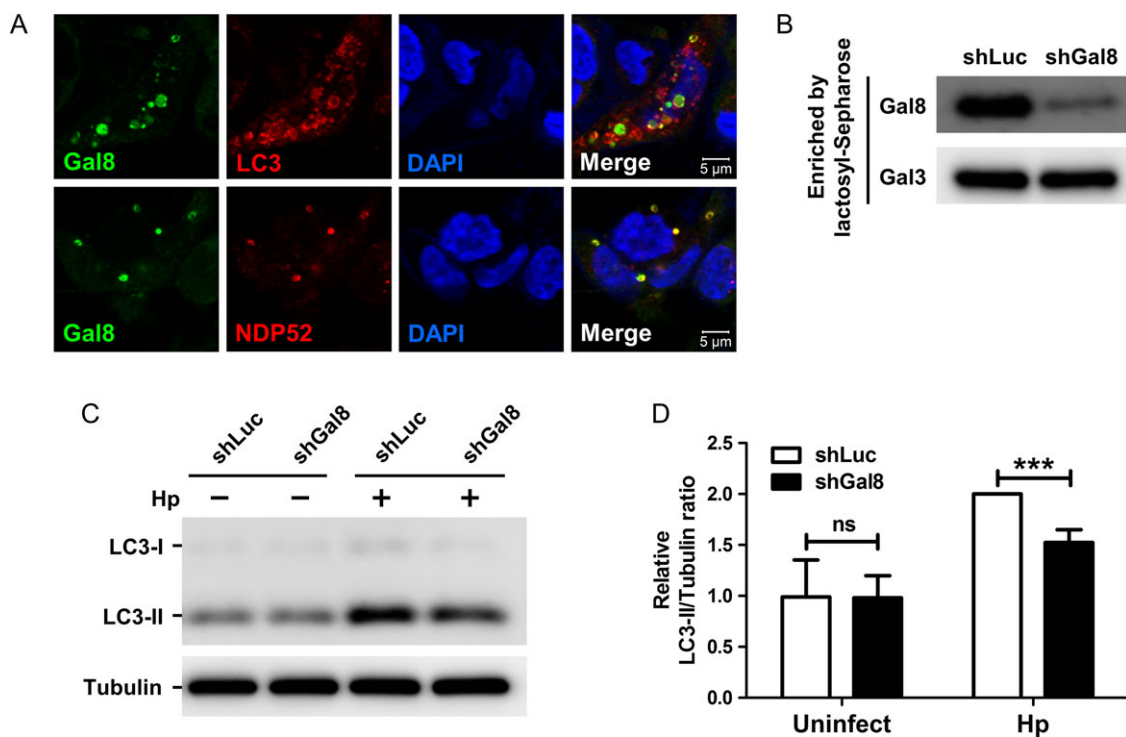


Fig. 3. Galectin-8 upregulates autophagy activity in *H. pylori*-infected cells. (A) After infection with *H. pylori* 26695 (moi = 400) for 6 h, cells were stained with anti-galectin-8, anti-NDP52 or anti-LC3 antibodies and appropriate fluorescence-labeled secondary antibodies. DAPI stains nuclei and bacteria. Scale bar, 5 μ m. Yellow color represents colocalization of galectin-8 with NDP52 and LC3, respectively. (B) Galectin-8 knockdown cells and control shLuc cells were lysed. Cell lysates were incubated with lactosyl-Sepharose. The bound proteins were eluted and immunoblotted with indicated antibodies. (C) Indicated cells were infected with *H. pylori* 26695 (moi = 400) for 6 h and treated with 10 nM bafilomycin A1 at the last 2 h, followed by immunoblot analysis. (D) Quantitative analysis of the relative amounts of LC3-II in indicated cells from four independent experiments as described in (C). Values represent means \pm SD. *** P < 0.001. ns, not significant. Hp, *H. pylori*.

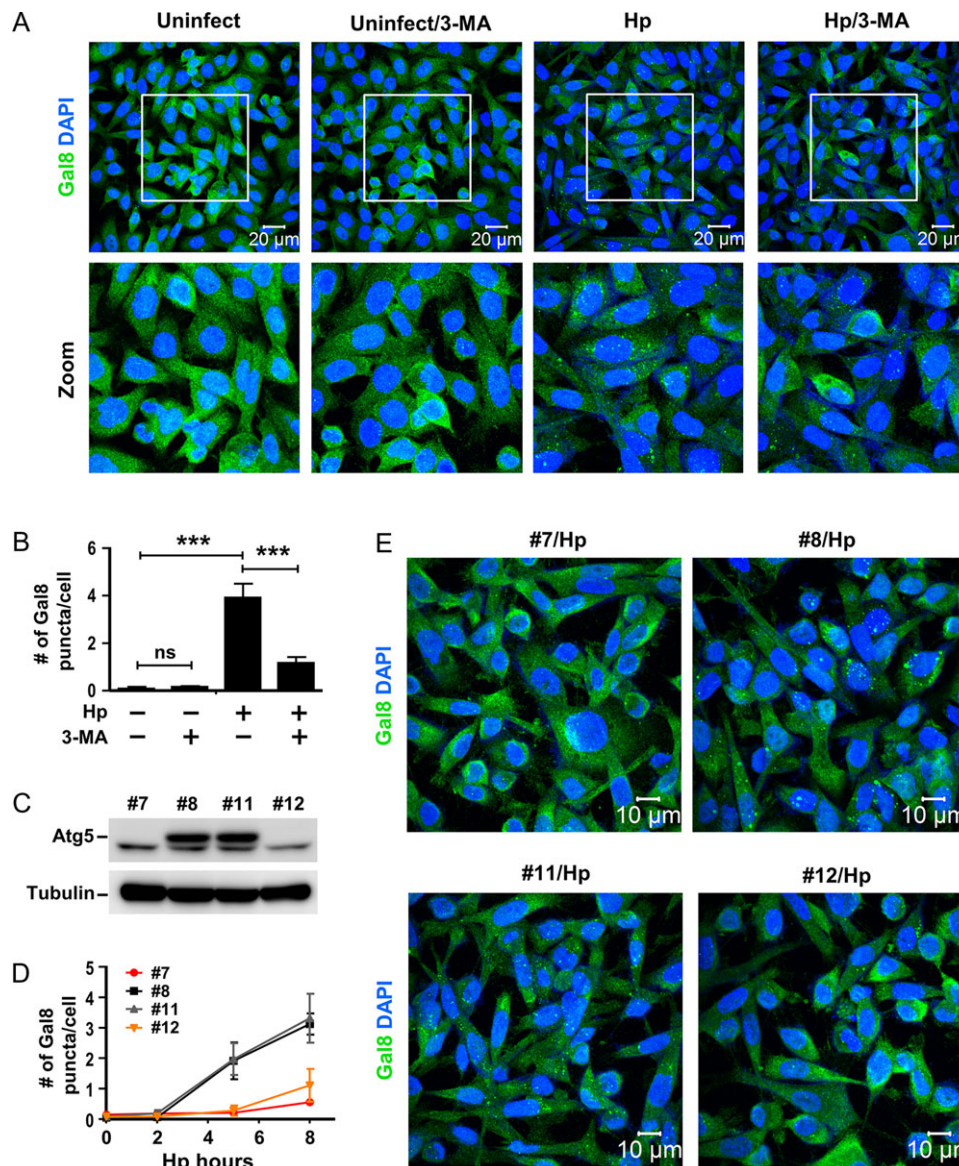


Fig. 4. Autophagy facilitates *H. pylori*-mediated galectin-8 aggregation. (A) Cells were pretreated with 5 mM 3-MA for 1 h and infected with *H. pylori* 26695 (moi = 400) for 8 h. Cells and bacteria were then stained as in Figure 1C. Scale bar, 20 μ m. (B) Quantitative analysis of galectin-8 puncta per cell from three independent experiments as described in (A). Values represent means \pm SD. (C) Different AGS wild-type or *atg5* knockout cell clones were lysed and immunoblotted with indicated antibodies. (D and E) Wild-type or *atg5* knockout cell clones were infected with *H. pylori* 26695 (moi = 400) for 2, 5 or 8 h. Cells and bacteria were then stained as in Figure 1C. The quantitative result of galectin-8 puncta per cell from three independent experiments is shown in (D). Values represent means \pm SD. Representative confocal images of cells infected for 8 h are shown in (E). Scale bar, 10 μ m. *** P < 0.001. 3-MA, 3-methyladenine; Hp, *H. pylori*; ns, not significant.

contributes to *H. pylori*-mediated galectin-8 aggregation. These results, together with those supporting a role for galectin-8 aggregates in *H. pylori*-mediated autophagy (Figure 3C and D), indicate a reciprocal regulation loop between galectin-8 aggregation and autophagy during *H. pylori* infection.

NDP52 knockdown reduces *H. pylori*-mediated galectin-8 aggregation

NDP52 mediates autophagy activation in response to endomembrane damage (Thurston et al. 2012; Falcon et al. 2018). Since autophagy potentiates *H. pylori*-induced galectin-8 aggregation (Figure 4B and D), we speculated that NDP52 may be involved in

this process. To address this, NDP52-knockdown cells were generated (Figure 5A); these cells presented lower levels of galectin-8 aggregation compared with control cells after infection (Figure 5B and C), indicating a role for NDP52 in the promotion of galectin-8 aggregation in infected cells. These results suggest that autophagy may induce *H. pylori*-mediated galectin-8 aggregation, at least in part, via NDP52.

VacA cytotoxin contributes to *H. pylori*-induced galectin-8 aggregation and autophagy upregulation

Based on the observation that intracellular galectin-8 aggregation is elevated in response to infection by *H. pylori* 26695 (Figure 1E), we investigated whether this phenomenon occurs in cells exposed to

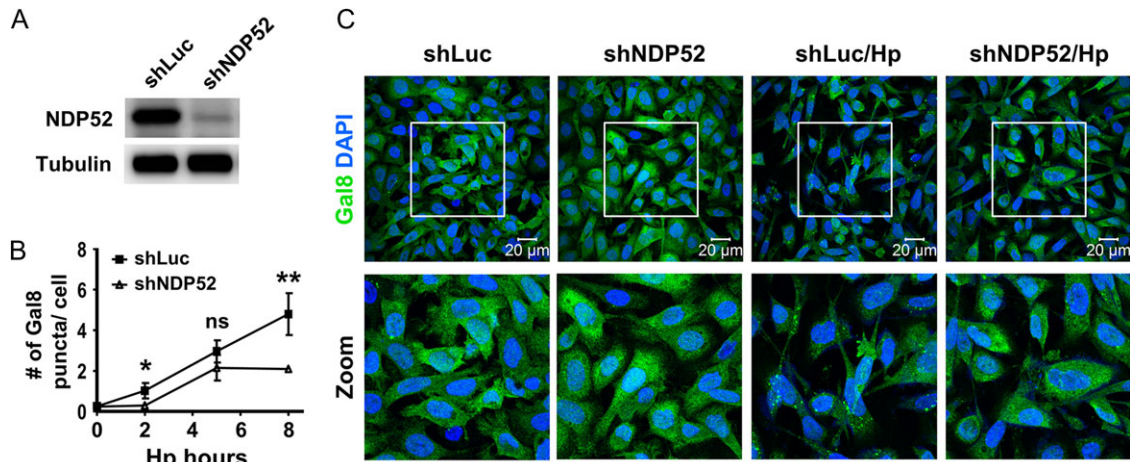


Fig. 5. NDP52 depletion reduces *H. pylori*-mediated galectin-8 aggregation. (A) AGS NDP52 knockdown cells and control shLuc cells were lysed and immunoblotted with anti-NDP52 and anti-tubulin antibodies. (B and C) Indicated cells were infected with *H. pylori* 26695 (moi = 200) for 2, 5 or 8 h and stained as in Figure 1C. The quantification of galectin-8 puncta per cell from four independent experiments is shown in (B). Values represent means \pm SD. Representative confocal images of cells infected for 8 h are shown in (C). Scale bar, 20 μ m. * P < 0.05, ** P < 0.01. Hp, *H. pylori*; ns, not significant.

other strains of *H. pylori*. Infection with another *H. pylori* strain, NCTC 11637, resulted in an increase in intracellular galectin-8 aggregation, and this effect was also diminished upon treatment with 3-MA (Figure 6A), which is consistent with our finding that autophagy upregulates galectin-8 aggregation in cells challenged by *H. pylori* 26695 (Figure 4B and D). VacA activates autophagy in gastric epithelial cells (Terebiznik et al. 2009). VacA deficiency in *H. pylori* strain NCTC 11637 reduced the increase in both LC3-II levels (Figure 6B) and intracellular galectin-8 aggregation (Figure 6C and D) upon infection. These results indicate that VacA contributes to *H. pylori*-mediated galectin-8 aggregation in a manner that is associated with autophagy upregulation.

Discussion

A novel finding of our study was that *H. pylori* infection triggers intracellular galectin-8 aggregation, which is dependent on host O-glycans and is associated with lysosomes. We hypothesize that *H. pylori* infection induces lysosomal damage in gastric epithelial cells, leading to the exposure of host glycans that are normally present in the lumen. We found that galectin-8 aggregation is dependent on autophagy, because it was diminished when autophagy was inhibited and when the expression of the autophagy adapter NDP52 was suppressed. Since we also showed that *H. pylori*-induced autophagy was dependent on the presence of galectin-8, our findings indicate the reciprocal regulation of galectin-8 aggregation and autophagy during infection. Finally, we found that VacA contributes to both increased autophagy and increased galectin-8 aggregation in infected cells, suggesting that this cytotoxin is the driving force for these two processes induced by *H. pylori*.

Galectins are cytosolic proteins, but can be secreted through an unknown mechanism (Hughes 1999); they exhibit both intracellular and extracellular functions. In recent years, cytosolic galectins have been shown to sense vacuole lysis via the detection of host glycans (Paz et al. 2010; Thurston et al. 2012). In those studies, intracellular bacteria, such as *S. typhimurium*, were found to disrupt endocytic vesicles, thereby exposing vacuolar luminal glycans to cytosolic galectins (-3, -8, and -9), leading to the development of intracellular galectin aggregates near damaged vesicles. As a consequence, galectins have been designated as novel markers of vacuolar rupture (Aits

et al. 2015). Other strategies have been developed to identify lysosomal damage, such as the detection of lysosomal cathepsins in the cytosol using enzymatic activity assays (Aits et al. 2015). We observed a mild but significant increase in cathepsin B enzymatic activity in digitonin-extracted cytosolic fractions after *H. pylori* infection (Figure 2B). This suggests that *H. pylori* ruptures a small portion of lysosomes or induces a low level of lysosomal leakage in infected cells. At any rate, we surmise that the host-glycan-dependent accumulation of galectin-8 around lysosomes provides strong evidence that *H. pylori* infection induces lysosomal damage, which in turn triggers galectin-8 aggregation.

Broken intracellular vesicles expose luminal glycans to the cytosolic milieu and thereby recruit galectins to these vesicles. By utilizing glycosylation inhibitors or cells with defects in glycosylation, several studies have implicated N- and O-glycans in galectin-3 aggregation upon bacterial invasion. *Shigella* infection fails to induce galectin-3 recruitment to internalized bacteria in CHO Lec1 cells lacking galactose-containing N-glycans (Paz et al. 2010). Kifunensine, a potent inhibitor of N-glycan processing, attenuates the accumulation of galectin-3 around intracellular *L. monocytogenes* (Weng et al. 2018), while cells treated with BGN, an O-glycosylation inhibitor, showed reduced galectin-3-mediated recruitment of guanylate binding proteins (GBPs) to *Yersinia pseudotuberculosis*-containing vesicles (Feeley et al. 2017). Hence, both N- and O-glycans are crucial for galectin-3 aggregation in response to vacuolar damage. In contrast, the contribution of N- and O-glycans to intracellular galectin-8 aggregation has not previously been documented. In the present study, we found compared with incubation with an N-linked glycosylation inhibitor, incubation with an O-linked glycosylation inhibitor remarkably decreased galectin-8-recognizable glycans from treated cells (Figure 2C) and suppressed galectin-8 aggregation in *H. pylori*-challenged cells (Figure 2D). This implies that O- rather than N-glycans are critical for *H. pylori*-mediated galectin-8 aggregation (Figure 7). Galectin-8 possesses two CRD domains; its N- and C-terminal CRD domains preferentially bind to α 2-3-linked sialic acid and N-acetylgalactosamine, respectively (Hirabayashi et al. 2002). Future investigation of terminal sialylation and galactosylation on N- and O-glycans in AGS cells may help clarify the differential requirement of these two types of glycans for galectin-8 aggregation upon *H. pylori* infection.

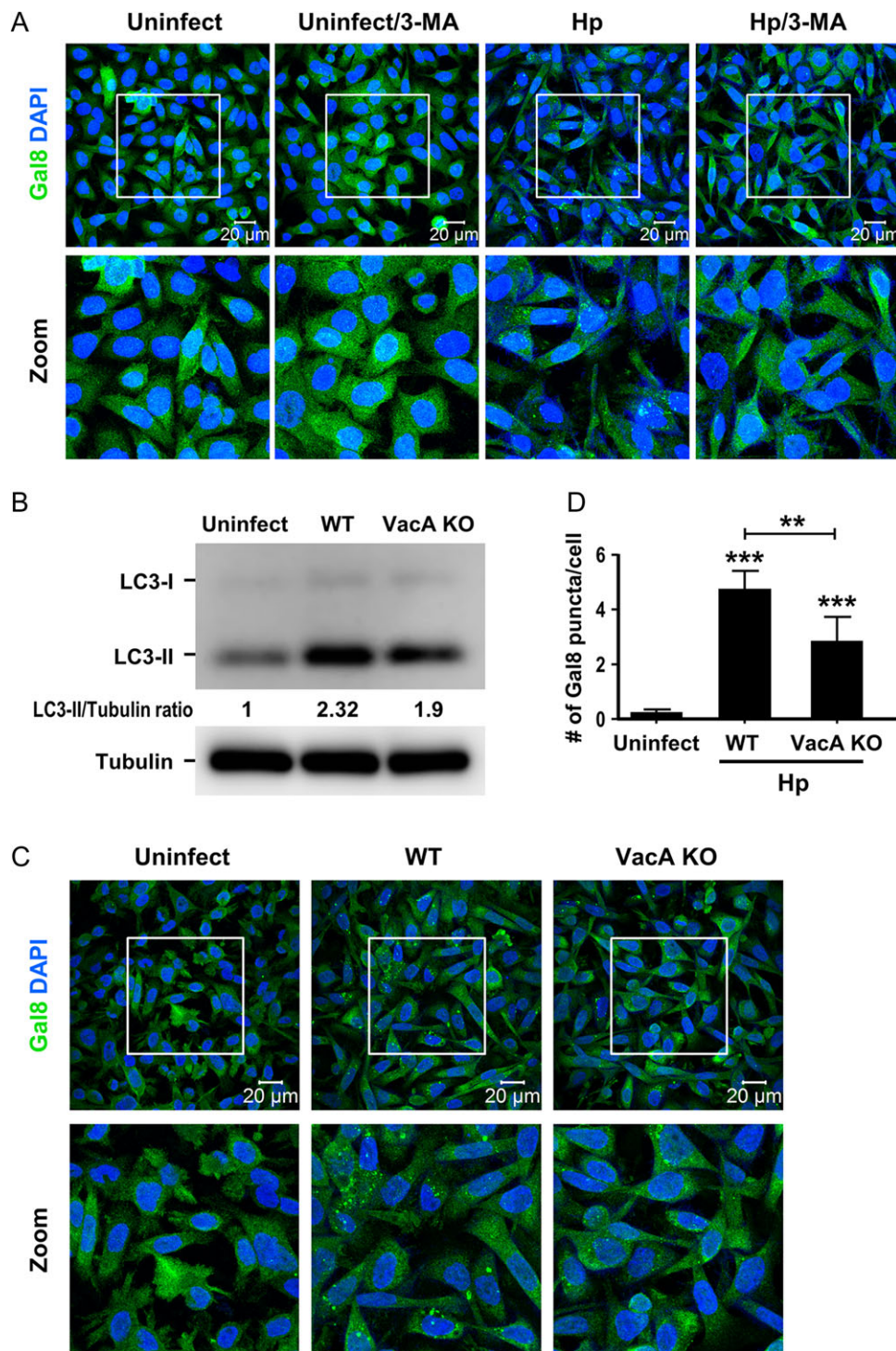


Fig. 6. VacA contributes to *H. pylori*-mediated autophagy and galectin-8 aggregation. (A) Cells were pretreated with 5 mM 3-MA for 1 h and then infected with *H. pylori* NCTC 11637 (moi = 200) for 8 h. Cells and bacteria were stained as in Figure 1C. Scale bar, 20 μ m. (B) Cells were infected with wild-type (WT) *H. pylori* NCTC 11637 or its VacA-knockout strain (moi = 200) for 8 h, and treated with 10 nM bafilomycin A1 at the last 2 h, followed by immunoblot analysis. The relative amounts of LC3-II are indicated. (C) Cells were infected as in (B). Cells and bacteria were stained as in Figure 1C. Scale bar, 20 μ m. (D) Quantitative analysis of galectin-8 puncta per cell from four independent experiments as described in (C). Values represent means \pm SD. ** P < 0.01, *** P < 0.001. 3-MA, 3-methyladenine.

During *H. pylori* infection, the accumulation of galectin-8 around damaged lysosomes promotes autophagy in infected cells (Figure 3C and D). This finding is consistent with that reported by

Thurston et al. (2012), who first showed that the recruitment of galectin-8 to ruptured endocytic vesicles activates autophagy. However, in contrast to their findings, we found a reciprocal

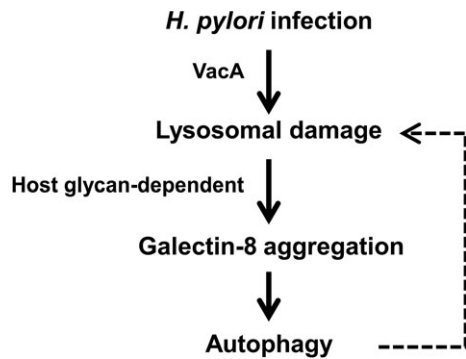


Fig. 7. A proposed model of regulation of galectin-8 aggregation in *H. pylori*-infected AGS cells. VacA compromises the integrity of lysosomal membrane during *H. pylori* infection. Ruptured lysosomes expose luminal contents to the cytosolic milieu. This enables the detection of luminal side of host glycans by cytosolic galectin-8, leading to galectin-8 aggregation around damaged lysosomes. These lysosome-accumulated galectin-8 aggregates enhance *H. pylori*-mediated autophagy. This functional effect on autophagy in turn expedites autophagy-driven lysosomal disruption and thus potentiates galectin-8 aggregation in infected cells.

regulation between galectin-8 aggregation and autophagy. Our observations support a function for autophagy in enhancing galectin-8 aggregation (Figure 4B and D), whereas the results of Thurston et al. indicated that autophagy is dispensable for vacuolar damage-induced galectin-8 aggregation. In fact, studies have shown that under some circumstances, autophagy facilitates lysosomal destabilization (Gonzalez et al. 2012; Wang et al. 2015; Hernandez-Tiedra et al. 2016; Yao et al. 2016; Liu et al. 2017; Wu et al. 2017). If this is true for *H. pylori*-infected AGS cells, lysosomal damage-mediated autophagy activation may accelerate the rate of lysosomal rupture through a feedback regulatory loop and result in a further increase in galectin-8 aggregation (Figure 7).

VacA is known to activate autophagy (Terebiznik et al. 2009). Indeed, compared with wild-type *H. pylori*, we observed that VacA-knockout derivatives elicited a reduced autophagy response (Figure 6B) in infected cells, and this was associated with a lower amount of galectin-8 aggregation (Figure 6C and D). Building on the present findings showing the reciprocal regulation of galectin-8 aggregation and autophagy in *H. pylori*-infected cells, we propose three possible mechanisms by which VacA affects galectin-8 aggregation. First, since VacA is a pore-forming toxin that may compromise the integrity of intracellular vesicles (Chitcholtan et al. 2008), it may directly destabilize the lysosomal membrane (Figure 7). This in turn facilitates galectin-8 accumulation and autophagy activation in infected cells. Second, VacA may contribute to *H. pylori*-mediated galectin-8 aggregation through the upregulation of autophagy. When mitochondria are damaged, lysosome-mediated degradation of defective mitochondria enhances the activity of the intralysosomal Fenton reaction, leading to the increased generation of hydroxyl radicals, which may disrupt lysosomes (Terman et al. 2008). VacA is known to impair mitochondrial function and reduce the mitochondrial membrane potential (Kimura et al. 1999). Therefore, a third possible mechanism is that VacA may promote lysosomal rupture-associated galectin-8 accumulation by damaging mitochondria.

In addition to VacA, other *H. pylori*-derived factors may modulate autophagy activity in infected cells. For example, a secreted antigen, HP0175, from *H. pylori* was reported to promote autophagy in gastric epithelial cells (Halder et al. 2015). Since *H. pylori*-mediated

autophagy activation facilitates intracellular galectin-8 aggregation in infected cells (Figure 4B and D), HP0175 may also potentiate galectin-8 aggregation by upregulating autophagy in infected cells. Additionally, because both HP0175 and VacA instigate autophagy by enhancing endoplasmic reticulum (ER) stress (Halder et al. 2015; Zhu et al. 2017), whether suppression of ER stress activity reduces autophagy-dependent galectin-8 aggregation in *H. pylori*-infected cells may warrant further study.

Several studies have revealed a change in galectin expression in AGS gastric epithelial cells in response to *H. pylori* exposure. mRNA levels of both galectin-1 and -3 have been shown to be upregulated in AGS cells stimulated with *H. pylori* (Lim et al. 2003). At the protein level, galectin-3 is augmented after infection (Subhash and Ho 2016). Regarding galectin-8, an increase in mRNA levels (Figure 1A) but a small reduction in protein extent (Figure 1B) was observed at 24 h postinfection. Herein, we postulate two possible mechanisms to explain this phenomenon. First, increased galectin-3 secretion was suggested to decrease intracellular galectin-3 (Laiko et al. 2010). Augmented galectin-8 secretion after *H. pylori* stimulation (Supplementary data, Figure S1A) may therefore reduce intracellular galectin-8 in host cells. Second, during lysosomal destruction, galectin-3 was reported to translocate into damaged lysosomes, followed by degradation via autophagy machinery (Maejima et al. 2013). Thus, galectin-8 on leaky lysosomes in *H. pylori*-infected cells might be degraded in an autophagy-dependent manner as well, leading to intracellular galectin-8 depletion after infection.

Galectin-3 is known to be able to associate with *H. pylori* (Fowler et al. 2006), and this interaction exhibits multiple effects on *H. pylori*, such as reduced bacterial growth (Park et al. 2016) and decreased adhesion to gastric epithelial cells (Subhash et al. 2016). Since galectin-8 can bind *H. pylori* (Supplementary data, Figure S1B), there is a great possibility that galectin-8 affects *H. pylori* viability and its adhesion to host cells as well. In addition to exerting these potential effects on *H. pylori*, extracellular galectin-8 was shown to activate immune cells. Galectin-8-treated dendritic cells display an activated phenotype and secrete more proinflammatory cytokines (Carabelli et al. 2017). Hence, *H. pylori*-driven increase in galectin-8 secretion (Supplementary data, Figure S1A) may contribute to *H. pylori*-induced gastric inflammation.

In conclusion, our study provides experimental evidence supporting an increase in lysosomal damage in gastric epithelial cells in response to *H. pylori* infection. While recognition of intracellular bacteria-mediated vacuolar destruction by galectins is well-illustrated (Chen et al. 2014), our findings indicate that galectin-8 senses lysosomal rupture induced by a noninvasive bacterium, *H. pylori*. In addition to host O-glycans, autophagy is critical for the augmentation of intracellular galectin-8 aggregation during *H. pylori* infection. To our knowledge, the regulation of galectin-8 aggregation by autophagy is so far unrecognized. We also demonstrated an involvement of VacA in *H. pylori*-elicited galectin-8 aggregation and autophagy activation. Since *H. pylori*-mediated autophagy may favor the development of gastric cancer (Diaz et al. 2018), our study also highlights a possible contribution of galectin-8 aggregation in *H. pylori*-infected gastric epithelial cells to gastric carcinogenesis.

Materials and methods

Cell culture and generation of NDP52 or galectin-8 knockdown cells

AGS cells, a human gastric epithelial cell line, were cultured in RPMI medium containing 10% heat-inactivated fetal bovine serum

(FBS) at 37°C in 5% CO₂. Lentivirus-encoded shRNAs were obtained from National RNAi Core Facility, Academia Sinica, Taiwan. The target sequences of NDP52 shRNA and galectin-8 shRNA are 5'-GAGCTGCTTCAACTGAAAGAA-3' and 5'-CCTGGAACCTTGGATTGTGATA-3', respectively. The target sequence of the negative-control luciferase shRNA (shLuc) is 5'-GCGGTTGCCAAGAGGTTCCAT-3'. To generate knockdown cells, AGS cells were incubated with shRNA-carrying lentivirus in the presence of polybrene (8 µg/mL) for 24 h, and infected cells were then selected by culture medium containing 2 µg/mL puromycin.

Generation of atg5 knockout cells by CRISPR-Cas9

To generate atg5 knockout AGS cells, CRISPR/Cas9-mediated genome editing technology was employed. All the CRISPR-related reagents, including the pAll-Cas9.pPuro expression vector, were derived from National RNAi Core Facility, Academia Sinica, Taiwan. Atg5 guide RNA (AACTTGTTCACGCTATATC) was cloned into the sgRNA expressing vector (pAll-Cas9.pPuro). After transfection into AGS cells, cells were treated with puromycin (2 µg/mL) for 4 days and then subjected to a BD FACSAria III cell sorter (Becton Dickinson) for isolation and separation of single cells. Atg5 knockout in single-cell clones was checked by immunoblot analysis.

Bacterial growth and infection

Helicobacter pylori wild-type strain 26695 (ATCC 700392), *H. pylori* wild-type strain NCTC 11637 (ATCC 43504), and its VacA-knockout mutant were used. *H. pylori* was cultured in brucella broth containing 10% FBS at 37°C under microaerophilic conditions. For infection, bacterial cells were harvested, resuspended in phosphate-buffered saline (PBS) and then added to AGS cells at the indicated multiplicity of infection (moi).

Quantitative PCR

Total RNA was extracted from AGS cells using Qiagen RNeasy Mini Kit according to the manufacturer's instructions. The cDNA was synthesized using iScript™ Reverse Transcription Supermix for RT-qPCR (Bio-Rad). Quantitative PCR was performed using a TaqMan assay and analyzed by the Bio-Rad CFX connect Real-Time system. The primers for human galectin-8 were as follows: forward 5'-TGCA CCAAATACCACCTATGA-3' and reverse 5'-CACTTCTCCTTAAAC GACGACA-3'. The relative mRNA expression of each sample was normalized against glyceraldehyde 3-phosphate dehydrogenase mRNA expression.

Drug treatment

Bafilomycin A1 (Sigma) was dissolved in dimethyl sulfoxide (DMSO, Sigma) and used at 10 nM. 3-MA (Merck) was dissolved in cell culture medium and used at 5 mM.

Fluorescence microscopy

Cells (2.5×10⁵ cells) were seeded overnight on coverslips in 24-well microtiter plates and then infected with *H. pylori* for indicated hours. After fixation with 4% paraformaldehyde (PFA) and subsequent permeabilization with 0.2% Triton X-100, cells were stained with anti-galectin-8 (R&D Systems), anti-EEA1 (Cell Signaling), anti-LAMP1 (Cell Signaling), anti-NDP52 (Abcam), and anti-LC3 (MBL) antibodies overnight at 4°C. After washing with PBS, cells were stained with Alexa Fluor-conjugated secondary antibodies and

DAPI (4', 6-diamidino-2-phenylindole) at room temperature for 1 h. Confocal images were captured by a Carl Zeiss LSM 700 laser scanning confocal microscope. The average number of galectin-8 puncta per cell was counted by using ImageJ software.

Immunoblot analysis

Cells were washed with PBS, and then lysed in lysis buffer (1% Triton X-100, 50 mM Tris at pH 7.4, 150 mM NaCl, 1 mM EDTA) supplemented with a protease inhibitor cocktail (Calbiochem). After centrifugation for 15 min at 15,000 rpm at 4°C, protein concentrations of the cell lysates were measured with Bio-Rad protein assay kit. Lysates were boiled in SDS-sample buffer, resolved in SDS polyacrylamide gel under reducing conditions, and transferred to PVDF membranes. The blots were incubated overnight at 4°C with primary antibodies, including anti-LC3 (Cell signaling), anti-atg5 (GeneTex), anti-NDP52 (Abcam), and anti-tubulin (Proteintech) antibodies, washed for three times, incubated with HRP-conjugated antibody for 1 h at room temperature, and then detected by ECL Prime Western Blotting Detection Reagent (Amersham). To enrich galectin proteins from cell lysates, 450 µg of cell lysates were incubated with lactosyl-Sepharose overnight at 4°C. Beads were then washed three times with lysis buffer and bound proteins were eluted with SDS-sample buffer. Following electrotransfer to PVDF membranes, anti-galectin-8 (Cusabio Biotech) and anti-galectin-3 (GeneTex) antibodies were used for detection.

Lectin binding

Cells were treated with 1 mM 1-deoxymannojirimycin (DMJ) (Toronto Research Chemicals) or 10 mM benzyl 2-acetamido-2-deoxy-α-D-galactopyranoside (BGN) (Sigma) for 24 h, and harvested by treatment with Cellstripper (Coring). After washing with PBS, cells were stained with different fluorescein isothiocyanate (FITC)-labeled lectins: Phaseolus Vulgaris Leucoagglutinin (PHA-L), Peanut Agglutinin (PNA) (Vector Laboratories), and recombinant human galectin-8 (R&D Systems). Samples were analyzed by FACS Canto flow cytometer (BD Biosciences). For determining *H. pylori*-binding potential of galectin-8, bacterial cells were resuspended in PBS, incubated with FITC-labeled recombinant galectin-8 in the presence of 25 mM sucrose or lactose, and then analyzed by flow cytometry.

ELISA (enzyme-linked immunosorbent assay) for galectin-8

96-well microplates were coated with an anti-galectin-8 capture antibody (R&D Systems) overnight at 4°C, washed with PBS containing 0.05% Tween 20, and blocked with assay diluent (eBioscience). The harvested culture supernatants were centrifuged at 350 ×g for 5 min and then added to precoated wells. After overnight incubation at 4°C, microplates were incubated with a biotinylated anti-galectin-8 detection antibody (R&D Systems) for 1 h at room temperature. After washing, microplates were incubated with avidin-linked horseradish peroxidase (BioLegend), followed with tetramethylbenzidine (TMB) substrate solution (BioLegend). The reaction was stopped by the addition of 1 M HCl, and the absorbance was measured at 450 nm by a Tecan Infinite M200 PRO plate reader.

Cathepsin B activity assay

After infection with *H. pylori* for 16 h, cells were washed and incubated with PBS containing 50 µg/mL digitonin for 15 min on ice.

The supernatants were collected as cytosolic fractions, and protein concentrations of the fractions were estimated with Bio-Rad protein assay kit. Cathepsin B activity was analyzed by a fluorometric assay kit (Biovision) according to the manufacturer's protocol. Equal amounts of cytosolic proteins from different samples were incubated with cathepsin B reaction buffer containing cathepsin B substrate Ac-RR-AFC at 37°C for 2 h. The fluorescence (excitation 400 nm/emission 505 nm) was measured in a Tecan Infinite M200 PRO plate reader. Fold-increase in cathepsin B activity was determined by comparing the relative fluorescence units with the levels of uninfected samples after subtracting the levels of background samples (digitonin extraction buffer).

Statistical analysis

Prism 5 software was used for all statistical results. Data derived from at least three independent experimental repeats were shown as means \pm SD. Student's *t*-test was used to determine the statistical differences between two groups. Analysis of multiple group data was performed by using one-way ANOVA. *P*-values < 0.05 indicate statistical significance.

Supplementary data

Supplementary data is available at *Glycobiology* online.

Acknowledgements

We thank the National RNAi Core Facility at Academia Sinica in Taiwan for providing shRNA reagents and related services.

Funding

This work was supported by grants from Academia Sinica and Ministry of Science and Technology under Grants: MOST 106-0210-01-15-02, MOST 107-0210-01-19-01, AS-105-TP-B05 and AS-105-TP-B08.

Conflict of interest statement

None declared.

Abbreviations

3-MA, 3-methyladenine; BGN, benzyl 2-acetamido-2-deoxy- α -D-galactopyranoside; CagA, cytotoxin-associated gene A; CRISPR, clustered regularly interspaced short palindromic repeats; DMJ, deoxymannojirimycin; EEA1, early endosome antigen 1; ER, endoplasmic reticulum; FITC, fluorescein isothiocyanate; Gal8, galectin-8; Hp, *Helicobacter pylori*; LAMP1, lysosomal-associated membrane protein 1; LC3, microtubule-associated protein light chain 3; moi, multiplicity of infection; NDP52, nuclear dot protein 52; PHA-L, phaseolus vulgaris leucoagglutinin; PNA, peanut agglutinin; ROS, reactive oxygen species; VacA, vacuolating cytotoxin A; WT, wild-type.

References

Aits S, Jaattela M. 2013. Lysosomal cell death at a glance. *J Cell Sci.* 126: 1905–1912.

Aits S, Jaattela M, Nylandsted J. 2015. Methods for the quantification of lysosomal membrane permeabilization: A hallmark of lysosomal cell death. *Methods Cell Biol.* 126:261–285.

Atherton JC. 2006. The pathogenesis of *Helicobacter pylori*-induced gastrointestinal diseases. *Annu Rev Pathol.* 1:63–96.

Backert S, Ziska E, Brinkmann V, Zimny-Arndt U, Fauconier A, Jungblut PR, Naumann M, Meyer TF. 2000. Translocation of the *Helicobacter pylori* CagA protein in gastric epithelial cells by a type IV secretion apparatus. *Cell Microbiol.* 2:155–164.

Bagriacik EU, Kirkpatrick A, Miller KS. 1996. Glycosylation of native MHC class Ia molecules is required for recognition by allogeneic cytotoxic T lymphocytes. *Glycobiology.* 6:413–421.

Barondes SH, Cooper DN, Gitt MA, Leffler H. 1994. Galectins. Structure and function of a large family of animal lectins. *J Biol Chem.* 269: 20807–20810.

Boya P, Kroemer G. 2008. Lysosomal membrane permeabilization in cell death. *Oncogene.* 27:6434–6451.

Carabelli J, Quattrocchi V, D'Antuono A, Zamorano P, Tribulatti MV, Campetella O. 2017. Galectin-8 activates dendritic cells and stimulates antigen-specific immune response elicitation. *J Leukoc Biol.* 102: 1237–1247.

Chen HY, Weng IC, Hong MH, Liu FT. 2014. Galectins as bacterial sensors in the host innate response. *Curr Opin Microbiol.* 17:75–81.

Chitcholtan K, Hampton MB, Keenan JI. 2008. Outer membrane vesicles enhance the carcinogenic potential of *Helicobacter pylori*. *Carcinogenesis.* 29:2400–2405.

de Bernard M, Arico B, Papini E, Rizzuto R, Grandi G, Rappuoli R, Montecucco C. 1997. *Helicobacter pylori* toxin VacA induces vacuole formation by acting in the cell cytosol. *Mol Microbiol.* 26:665–674.

Delgado M, Singh S, De Haro S, Master S, Ponpuak M, Dinkins C, Ornatowski W, Vergne I, Deretic V. 2009. Autophagy and pattern recognition receptors in innate immunity. *Immunol Rev.* 227:189–202.

Deretic V, Saitoh T, Akira S. 2013. Autophagy in infection, inflammation and immunity. *Nat Rev Immunol.* 13:722–737.

Diaz P, Valenzuela Valderrama M, Bravo J, Quest AFG. 2018. *Helicobacter pylori* and gastric cancer: Adaptive Cellular Mechanisms Involved in Disease Progression. *Front Microbiol.* 9:5.

Falcon B, Noad J, McMahon H, Randow F, Goedert M. 2018. Galectin-8-mediated selective autophagy protects against seeded tau aggregation. *J Biol Chem.* 293:2438–2451.

Feeley EM, Pilla-Moffett DM, Zwack EE, Piro AS, Finethy R, Kolb JP, Martinez J, Brodsky IE, Coers J. 2017. Galectin-3 directs antimicrobial guanylate binding proteins to vacuoles furnished with bacterial secretion systems. *Proc Natl Acad Sci U S A.* 114:E1698–E1706.

Figueiredo C, Machado JC, Pharoah P, Seruca R, Sousa S, Carvalho R, Capelinha AF, Quint W, Caldas C, van Doorn LJ et al. 2002. *Helicobacter pylori* and interleukin 1 genotyping: An opportunity to identify high-risk individuals for gastric carcinoma. *J Natl Cancer Inst.* 94: 1680–1687.

Filomeni G, De Zio D, Cecconi F. 2015. Oxidative stress and autophagy: The clash between damage and metabolic needs. *Cell Death Differ.* 22: 377–388.

Fowler M, Thomas RJ, Atherton J, Roberts IS, High NJ. 2006. Galectin-3 binds to *Helicobacter pylori* O-antigen: It is upregulated and rapidly secreted by gastric epithelial cells in response to *H. pylori* adhesion. *Cell Microbiol.* 8:44–54.

Gonzalez P, Mader I, Tchoghandjian A, Enzenmuller S, Cristofanon S, Basit F, Debatin KM, Fulda S. 2012. Impairment of lysosomal integrity by B10, a glycosylated derivative of betulinic acid, leads to lysosomal cell death and converts autophagy into a detrimental process. *Cell Death Differ.* 19:1337–1346.

Halder P, Datta C, Kumar R, Sharma AK, Basu J, Kundu M. 2015. The secreted antigen, HP0175, of *Helicobacter pylori* links the unfolded protein response (UPR) to autophagy in gastric epithelial cells. *Cell Microbiol.* 17:714–729.

Hernandez-Tiedra S, Fabrias G, Davila D, Salanueva JJ, Casas J, Montes LR, Anton Z, Garcia-Taboada E, Salazar-Roa M, Lorente M et al. 2016. Dihydroceramide accumulation mediates cytotoxic autophagy of cancer cells via autolysosome destabilization. *Autophagy.* 12:2213–2229.

Hirabayashi J, Hashidate T, Arata Y, Nishi N, Nakamura T, Hirashima M, Urashima T, Oka T, Futai M, Muller WE et al. 2002. Oligosaccharide

- specificity of galectins: A search by frontal affinity chromatography. *Biochim Biophys Acta*. 1572:232–254.
- Huff JL, Hansen LM, Solnick JV. 2004. Gastric transcription profile of *Helicobacter pylori* infection in the rhesus macaque. *Infect Immun*. 72: 5216–5226.
- Hughes RC. 1999. Secretion of the galectin family of mammalian carbohydrate-binding proteins. *Biochim Biophys Acta*. 1473:172–185.
- Izzotti A, De Flora S, Cartiglia C, Are BM, Longobardi M, Camoirano A, Mura I, Dore MP, Scanu AM, Rocca PC et al. 2007. Interplay between *Helicobacter pylori* and host gene polymorphisms in inducing oxidative DNA damage in the gastric mucosa. *Carcinogenesis*. 28:892–898.
- Jia J, Abudu YP, Claude-Taupin A, Gu Y, Kumar S, Choi SW, Peters R, Mudd MH, Allers L, Salemi M et al. 2018. Galectins control mTOR in response to endomembrane damage. *Mol Cell*. 70:120–135 e128.
- Jones KR, Whitmire JM, Merrell DS. 2010. A tale of two toxins: *Helicobacter pylori* CagA and VacA modulate host pathways that impact disease. *Front Microbiol*. 1:115.
- Kaur J, Debnath J. 2015. Autophagy at the crossroads of catabolism and anabolism. *Nat Rev Mol Cell Biol*. 16:461–472.
- Kim IJ, Lee J, Oh SJ, Yoon MS, Jang SS, Holland RL, Reno ML, Hamad MN, Maeda T, Chung HJ et al. 2018. *Helicobacter pylori* infection modulates host cell metabolism through VacA-dependent inhibition of mTORC1. *Cell Host Microbe*. 23:583–593 e588.
- Kimura M, Goto S, Wada A, Yahiro K, Niidome T, Hatakeyama T, Aoyagi H, Hirayama T, Kondo T. 1999. Vacuolating cytotoxin purified from *Helicobacter pylori* causes mitochondrial damage in human gastric cells. *Microb Pathog*. 26:45–52.
- Laiko M, Murtazina R, Malyukova I, Zhu C, Boedeker EC, Gutsal O, O'Malley R, Cole RN, Tarr PI, Murray KF et al. 2010. Shiga toxin 1 interaction with enterocytes causes apical protein mistargeting through the depletion of intracellular galectin-3. *Exp Cell Res*. 316:657–666.
- Lim JW, Kim H, Kim KH. 2003. Cell adhesion-related gene expression by *Helicobacter pylori* in gastric epithelial AGS cells. *Int J Biochem Cell Biol*. 35:1284–1296.
- Liu FT, Yang RY, Hsu DK. 2012. Galectins in acute and chronic inflammation. *Ann N Y Acad Sci*. 1253:80–91.
- Liu L, Zhang N, Dou Y, Mao G, Bi C, Pang W, Liu X, Song D, Deng H. 2017. Lysosomal dysfunction and autophagy blockade contribute to IMB-6G-induced apoptosis in pancreatic cancer cells. *Sci Rep*. 7: 41862.
- Maejima I, Takahashi A, Omori H, Kimura T, Takabatake Y, Saitoh T, Yamamoto A, Hamasaki M, Noda T, Isaka Y et al. 2013. Autophagy sequesters damaged lysosomes to control lysosomal biogenesis and kidney injury. *EMBO J*. 32:2336–2347.
- Mizushima N. 2007. Autophagy: Process and function. *Genes Dev*. 21: 2861–2873.
- Odenbreit S, Puls J, Sedlmaier B, Gerland E, Fischer W, Haas R. 2000. Translocation of *Helicobacter pylori* CagA into gastric epithelial cells by type IV secretion. *Science*. 287:1497–1500.
- Palfaman SL, Kwok T, Gabriel K. 2012. Vacuolating cytotoxin A (VacA), a key toxin for *Helicobacter pylori* pathogenesis. *Front Cell Infect Microbiol*. 2:92.
- Park AM, Hagiwara S, Hsu DK, Liu FT, Yoshie O. 2016. Galectin-3 plays an important role in innate immunity to gastric infection by *Helicobacter pylori*. *Infect Immun*. 84:1184–1193.
- Paz I, Sachse M, Dupont N, Mounier J, Cederfur C, Enninga J, Leffler H, Poirier F, Prevost MC, Lafont F et al. 2010. Galectin-3, a marker for vacuole lysis by invasive pathogens. *Cell Microbiol*. 12:530–544.
- Subhash VV, Ho B. 2016. Galectin 3 acts as an enhancer of survival responses in *H. pylori*-infected gastric cancer cells. *Cell Biol Toxicol*. 32:23–35.
- Subhash VV, Ling SS, Ho B. 2016. Extracellular galectin-3 counteracts adhesion and exhibits chemoattraction in *Helicobacter pylori*-infected gastric cancer cells. *Microbiology*. 162:1360–1366.
- Suzuki O, Abe M. 2014. Galectin-1-mediated cell adhesion, invasion and cell death in human anaplastic large cell lymphoma: Regulatory roles of cell surface glycans. *Int J Oncol*. 44:1433–1442.
- Terebiznik MR, Raju D, Vazquez CL, Torbrick K, Kulkarni R, Blanke SR, Yoshimori T, Colombo MI, Jones NL. 2009. Effect of *Helicobacter pylori*'s vacuolating cytotoxin on the autophagy pathway in gastric epithelial cells. *Autophagy*. 5:370–379.
- Terman A, Kurz T, Gustafsson B, Brunk UT. 2008. The involvement of lysosomes in myocardial aging and disease. *Curr Cardiol Rev*. 4:107–115.
- Thurston TL, Wandel MP, von Muhlinen N, Foeglein A, Randow F. 2012. Galectin 8 targets damaged vesicles for autophagy to defend cells against bacterial invasion. *Nature*. 482:414–418.
- Walczak M, Martens S. 2013. Dissecting the role of the Atg12-Atg5-Atg16 complex during autophagosome formation. *Autophagy*. 9:424–425.
- Wang Y, Liu Y, Liu X, Jiang L, Yang G, Sun X, Geng C, Li Q, Yao X, Chen M. 2015. Citreoviridin induces autophagy-dependent apoptosis through lysosomal-mitochondrial axis in human liver HepG2 cells. *Toxins (Basel)*. 7:3030–3044.
- Weng IC, Chen HL, Lo TH, Lin WH, Chen HY, Hsu DK, Liu FT. 2018. Cytosolic galectin-3 and -8 regulate antibacterial autophagy through differential recognition of host glycans on damaged phagosomes. *Glycobiology*. 28:392–405.
- Wu X, Jiang L, Sun X, Yao X, Bai Y, Liu X, Liu N, Zhai X, Wang S, Yang G. 2017. Mono(2-ethylhexyl) phthalate induces autophagy-dependent apoptosis through lysosomal-mitochondrial axis in human endothelial cells. *Food Chem Toxicol*. 106:273–282.
- Yang Z, Klionsky DJ. 2010. Mammalian autophagy: Core molecular machinery and signaling regulation. *Curr Opin Cell Biol*. 22:124–131.
- Yao X, Sha S, Wang Y, Sun X, Cao J, Kang J, Jiang L, Chen M, Ma Y. 2016. Perfluorooctane sulfonate induces autophagy-dependent apoptosis through Spinster 1-mediated lysosomal-mitochondrial axis and impaired mitophagy. *Toxicol Sci*. 153:198–211.
- Zhu P, Xue J, Zhang ZJ, Jia YP, Tong YN, Han D, Li Q, Xiang Y, Mao XH, Tang B. 2017. *Helicobacter pylori* VacA induces autophagic cell death in gastric epithelial cells via the endoplasmic reticulum stress pathway. *Cell Death Dis*. 8:3207.